Hot-carrier energy-loss rates in $GaAs/Al_xGa_{1-x}As$ quantum wells

K. Leo, W. W. Rühle, and K. Ploog
Max-Planck-Institut für Festkörperforschung, Heisenbergstrasse 1, Postfach 80 06 65, D-7000 Stuttgart 80, Federal Republic of Germany
(Received 19 January 1988)

We present a systematic study of the cooling of hot carriers in undoped, *n*-type doped, and *p*-type doped $GaAs/Al_xGa_{1-x}As$ quantum wells of different well widths by time-resolved luminescence spectroscopy. The energy loss of the carriers due to interaction with optical phonons is independent of dimensionality and well width. The energy loss of electrons is highly reduced at all excitation densities compared with a simple theory of the interactions; for holes, the energy loss comes close to theory at low excitation density. The reduction of the energy-loss rate by optical-phonon scattering cannot be explained by screening or degeneracy but rather is consistent with a hot-phonon effect. The energy-loss rate due to deformation-potential scattering with acoustical phonons increases with decreasing well width.

I. INTRODUCTION

The electronic transport properties of GaAs and $Al_xGa_{1-x}As/GaAs$ heterostructures are determined over a wide range of carrier temperatures by scattering with phonons. The electron-phonon interaction in polar semiconductors was frequently studied by tracing the cooling of a hot, laser-generated electron-hole plasma with time-resolved luminescence.[1] At temperatures ≥ 45 K this cooling process is determined by the emission of polar optical phonons due to the Fröhlich interaction.[2] In bulk GaAs as well as in $GaAs/Al_xGa_{1-x}As$ quantum wells (QW's), the experiments generally yield a strongly reduced cooling at higher excitation densities compared to a simple theory of the Fröhlich interaction, which assumes no screening and a phonon population corresponding to the lattice temperature.

This discrepancy between experiments and the simple theory has been discussed intensely in the last years.[1,3] Proposed explanations are (i) screening of the long-range Fröhlich interaction by the high carrier density,[4] (ii) a buildup of nonthermalized ("hot") LO phonons at the wave vectors most strongly involved in the interaction with the carriers, leading to reabsorption of phonons by the electron-hole plasma (EHP),[5,6] (iii) a reduction of the scattering rate of the EHP with the optical phonons due to the degeneracy of the carriers at high densities and low temperatures,[7] and (iv) the influence of plasmon-phonon coupling on the energy-loss rate (ELR).[8,9] It has been argued that a combination of two or more of these effects must be taken into account to explain the experimental observations.[5,6,8,10]

A topic of great current interest is the influence of the reduced dimensionality of thin crystal layers on this scattering rate.[3] The situation in two-dimensional (2D) systems is even more complicated than in three-dimensional (3D) systems. Theoretical calculations predict only a minor influence of the reduced dimensionality or the well width on the electron-phonon coupling.[11-13] The existence of a hot-phonon effect similar to that expected for bulk GaAs has been proposed by several authors.[8,12-14]

The ELR in 2D systems was studied experimentally by several groups,[15-33] and the results are very contradictory: For instance, an influence of dimensionality and QW thickness was stated[16,17,21,23,29] or denied,[22,26-28,30,31,33] or a time dependence[22] or independence[25,26,30,31] of the ELR reduction was claimed.

In this paper, we present investigations of the cooling of a hot EHP in undoped, *n*-type doped and *p*-type doped QW. We discuss in detail the shape of the transient spectra and how density and temperature are determined from these spectra. The necessary improvements of the theoretical fit procedure of cooling curves to the experimental data are described. The essential experimental results are as follows. (i) The ELR by polar optical scattering (PO ELR) in bulk GaAs and in QW's of various well widths is strongly dependent on excitation density. It is *independent* of dimensionality and well width, if the *sheet* carrier density is used as parameter. (ii) The cooling of electrons and holes is different: In *n*-type doped QW's, the PO ELR is reduced by more than an order of magnitude even under weak excitation. In *p*-type doped QW's, however, the PO ELR reaches the prediction of the simple theory of the Fröhlich interaction at low excitation density. At high excitation density, both dopings have a similar behavior. It thus turns out that screening and degeneracy have no major influence of the PO ELR. (iii) A simple model for a 2D hot-phonon effect is developed and describes quite well the experimental observations. (iv) The cooling by acoustical deformation-potential (ADP) scattering at low temperatures (<45 K) depends on the well width: A wide QW (20-nm thick) shows about the same ADP ELR as bulk GaAs; in narrow QW's, the ADP ELR increases.

Finally, we compare our results with the literature and show that most of the contradictory results can be resolved by a thorough discussion of the experimental findings using more sophisticated fitting procedures.

 ©1988 The American Physical Society

II. EXPERIMENT

A. Samples and experimental setup

The undoped (residual carrier density below 10^{15} cm^{-3}) multiple-quantum-well (MQW) structures consist of 20 undoped GaAs layers of 3-, 9-, and 20-nm nominal width, respectively, clad by 35-nm-thick $Al_{0.34}Ga_{0.66}As$ barrier layers grown by molecular-beam epitaxy on semi-insulating (001)-oriented GaAs substrates. The modulation-doped MQW's consist of ten GaAs layers, clad by two undoped 13-nm-thick $Al_{0.34}Ga_{0.66}As$ barrier layers sandwiching a 9-nm-thick Si- (n-type) or Be- (p-type) doped $Al_{0.34}Ga_{0.66}As$ layer. The bulk GaAs sample consists of a 0.2-μm undoped GaAs layer clad by thick ($d > 1$ μm) $Al_{0.4}Ga_{0.6}As$ layers grown by liquid-phase epitaxy on semi-insulating GaAs substrate. The sample data are compiled in Table I.

The samples are mounted on the cold finger of a He cryostat having a temperature lower than 10 K. The plasma reaches after long delay time (> 1 ns) temperatures as low as about 20 K. Heating effects, which could influence the results of this study,[34] can therefore be excluded. The samples are excited by an argon-ion laser pumped synchronously mode-locked dye laser with a repetition rate of 80 MHz and a pulse length [full width at half maximum (FWHM)] of 4 ps. Styril-9, Pyridin-2, and DCM are used as dyes, giving a tunability range between 840 and 620 nm with an average power in the range of 40–80 mW. The luminescence is focused on the vertical entrance slit of a 0.32-m monochromator. The grating of the monochromator is partly covered to reduce the temporal dispersion of the system. The exit slit of the monochromator is replaced by a Hamamatsu 2D streak camera with a horizontal entrance slit. The luminescence intensity as a function of time and photon energy is read out simultaneously by a silicon-intensified-target (SIT) camera and can be analyzed by a digital image processor. The overall time resolution of the system including the temporal dispersion of the monochromator is below 20 ps. The spectral resolution is about 1.5 meV.

The photon energy of the laser is tuned for all experiments with the QW's to about 0.12 eV above the $n=1$ electron- to heavy-hole transition determined from the photoluminescence excitation spectra of the undoped samples. In case of the bulk sample, we use the same excess energy relative to the luminescence maximum in the low-excitation limit. Measurements with excess energies between 0.1 and 0.2 eV indicated only a weak dependence of the cooling process on the excess energy. In all our measurements the photons are absorbed in the GaAs layers only, thus avoiding heating effects due to the delayed trapping of carriers created in the $Al_xGa_{1-x}As$ barriers. Such heating effects can significantly modify the experimental findings in hot-carrier cooling experiments.[23] The total thickness of the GaAs layers used is small enough to ensure a nearly homogeneous excitation in depth. The density change with delay time due to lateral diffusion can be neglected for our laser-focus diameters (> 15 μm); however, the density is not constant, but varies across a diameter with a Gaussian profile. The excitation density is varied by choosing an appropriate focus diameter by defocusing the laser. The focus diameter is measured with a 5-μm pinhole. The carrier density can be calculated from the measured laser power and focus diameter (FWHM), and the absorption coefficients given in the literature for bulk GaAs (Ref. 35) and GaAs QW's.[36] A comparison with densities determined by analysis of the luminescence spectra is given in Sec. II C.

B. Sample characterization

The luminescence and absorption properties of the QW samples are investigated by photoluminescence (PL) and photoluminescence excitation spectroscopy (PLE). The samples are excited with the pulsed laser at very low carrier densities ($\ll 10^{10}$ cm^{-2}); the time-integrated luminescence is detected with a photon-counting system. For the n-type modulation-doped MQW, the onset of the PLE intensity allow us to determine the doping density. The values obtained are, within error, in agreement with the densities determined by Hall-effect measurements which are given in Table I.

The PLE spectra reveal the energy of the subband edges. This information allows us to discuss the possible influence of transitions between higher subbands on our time-resolved measurements. For the 3- and the 9-nm QW's, we excite below the $n=2$ heavy-hole and light-hole–to–electron transitions; the Fermi levels are far

TABLE I. Data of the different QW samples. The densities and mobilities were obtained by Hall measurements at 4 K with weak illumination. The QW widths are nominal values. (und. denotes undoped.)

Sample	L_z (nm)	Type	Density (cm^{-2})	Mobility [cm^2 $(V s)^{-1}$]
A	20	n	8.0×10^{11}	3.4×10^{4}
B	20	p	6.0×10^{11}	2.2×10^{4}
C	9	n	1.2×10^{12}	7.0×10^{4}
D	9	p	4.5×10^{11}	9.1×10^{3}
E	3	n	6.2×10^{11}	5.3×10^{3}
F	3	p	5.0×10^{11}	3.3×10^{3}
G	20	und.		
H	9	und.		
I	3	und.		

below the $n=2$ subband edges at the excitation densities used in this experiment. We therefore avoid the influence of intersubband relaxation processes on the cooling of the hot carriers. In case of the 20-nm QW, however, the photons are absorbed in the $n=1$ to $n=3$ subbands. The Fermi level is for the highest excitation density in this QW above the $n=2$ subband edge. The influence of the higher subbands on the cooling of the hot carriers is discussed in Sec. IV A.

C. Determination of carrier temperatures and densities

The temperature T_C of the hot EHP can be deduced from the slope of the high-energy tail of the luminescence spectrum. The intensity I varies with the photon energy $h\nu$ as

$$I \propto \exp(-h\nu/kT_C) \ . \tag{1}$$

The carrier temperature determines the slope of the luminescence intensity plotted semilogarithmically as a function of $h\nu$. Figure 1 shows some typical results for different delay times. The carrier density can be obtained by analyzing the luminescence spectra with a more sophisticated model. We use a model similar to that given by Tränkle *et al.*:[37] The calculation assumes constant matrix element and k conservation for the recombination process; the carrier-carrier interaction is accounted for by a Landsberg-type broadening[38] of the electron states. The intensity $I(h\nu)$ is then given by

$$I(h\nu)=\sum_{i,j} m_i m_j f\left[\frac{h\nu}{1+m_i/m_j},\eta_e\right] f\left[\frac{h\nu}{1+m_j/m_i},\eta_h\right] \times \int_{E_i^0}^{\infty} dE\, L(E,h\nu,E_{\mathrm{land}}) \ , \tag{2}$$

where i and j are the subband indexes, f is the Fermi-Dirac distribution, E_i^0 is the edge of the ith subband, $m_{i,j}$ are the effective masses of electrons and holes, $\eta_{e,h}$ are the reduced Fermi energies for electrons and holes, respectively, and L is a Landsberg broadening function with E_{land} as broadening parameter. The subband energies needed for the calculations are derived from the transition energies measured by PLE spectroscopy. The carrier temperature determines the high-energy slope and the carrier density the width of the spectra. The dotted line in Fig. 2 shows the result of a fit in comparison with the transient spectrum of a 20-nm QW (solid line). The fit describes the general features of the spectrum well, but it does not cover the intensity decrease between the luminescence maximum and the kink at the Fermi level observed frequently in the spectra of QW's.[22,26] Possible explanations are (i) that the matrix element of recombination is, in contrast to our assumption, not energy independent, and (ii) that the Gaussian intensity profile of the laser beam (causing a laterally inhomogeneous density) leads to an overlap of spectra of different excitation density. A theoretical calculation[39] for an 18-nm QW gives in fact a reduction of the matrix element for increasing energy relative to the subband edge. The inhomogeneity can be approximated by adding several spectra calculated with different densities (in our calculation we used two spectra, the second one with a density reduced by 50%). If we include both effects into the calculation, we get a good fit (dashed line in Fig. 2). The disagreement at the low-energy shoulder is caused by substrate luminescence. The effect of the inhomogeneous density should be reduced if the doping density exceeds the excitation density, leading to a homogeneous density of one carrier type. By comparison of spectra with excitation density higher or lower than the doping density, we can investigate the influence of the inhomogeneous excitation. Figure 3 shows spectra of the different 9-nm QW's. In the undoped and p-type doped cases, where $n_{\mathrm{exc}}=p_{\mathrm{exc}}>p_0$, the spectra are described well (dashed lines), if an inhomogeneous density and the energy dependence of the matrix element are included. For the n-type doped sample, where $n_{\mathrm{exc}}<n_0$, the calculation without inhomogeneous density (dotted line) describes the experimental result best. This demonstrates that the inhomo-

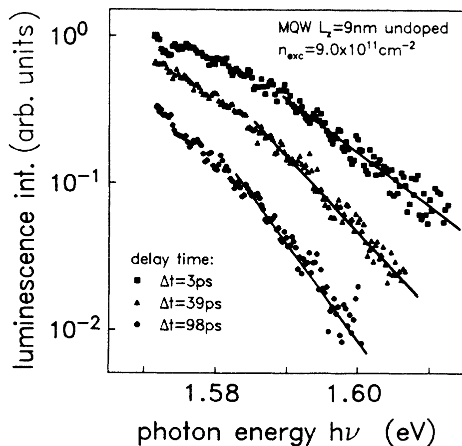

FIG. 1. Transient high-energy luminescence tails for an undoped 9-nm-thick MQW at the highest excitation density of 9×10^{12} cm^{-2} at various delay times ($t=0$ is set to 20 ps after the maximum of the laser pulse).

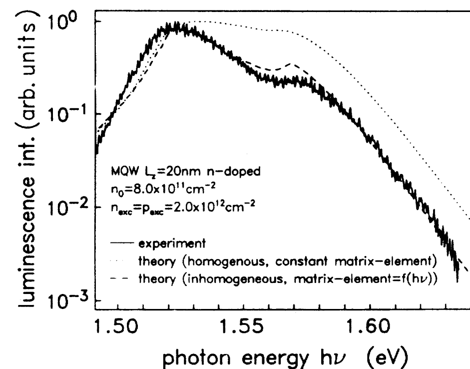

FIG. 2. Luminescence spectrum of an n-type doped 20-nm QW (solid line) compared to theoretical fits using the model described in the text. The best fit is obtained using energy-dependent matrix elements and inhomogeneous plasma density.

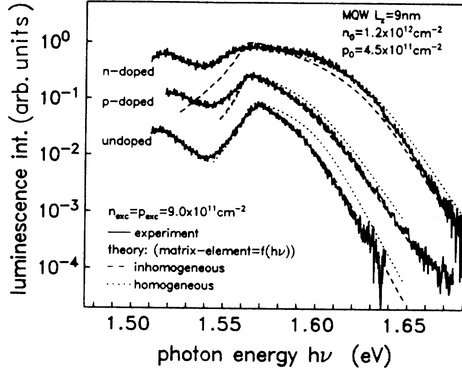

FIG. 3. Luminescence spectra of n-type doped (top), p-type doped (middle), and undoped (bottom) 9-nm MQW's in comparison to theoretical fits. The spectra of the undoped and of the p-type doped QW's, where the excitation density exceeds the doping density, is best described assuming inhomogeneous excitation density; the spectrum of the n-type doped QW, where the (homogeneous) doping density exceeds the excitation density, is better fitted assuming homogeneous density of the plasma. The peaks at 1.52 eV are caused by the luminescence of the bulk GaAs substrate.

geneous excitation profile of the laser actually influences the shape of the luminescence spectra. These effects exert, however, only a minor influence on the accuracy of the temperature determination. In particular, the matrix element is independent of energy at higher photon energies, i.e., in those parts of the spectra from which we determine the carrier temperature.

On the other hand, the energy dependence of the transition matrix element results in a heating effect, since carriers with lower energy recombine more rapidly than carriers with higher energy. We do not include this effect in our analysis since nonradiative recombination might prevail in our samples; in this case hot carriers recombine faster than cold carriers due to their higher thermal velocity.[40] We are thus not able to quantify these heating or cooling effects; however, we expect them to be negligible, since all carrier lifetimes involved are still reasonably longer than the cooling times.

The excitation densities deduced by a fit of the spectra are about a factor of 2 lower than the calculated densities. In this paper, we will use the density obtained by the fit procedure. The conclusions of our earlier publications,[30,31] where we used the calculated densities, are unchanged, since they rely on *relative* densities, and the relative density of different measurements or samples is known very accurately. The use of the lower-density values for analysis of the cooling curves leads to slight changes at the highest excitation density, mainly due to the density dependence of recombination heating.

III. ANALYSIS OF COOLING CURVES

The carrier temperatures at different delay times yield the cooling curve of the plasma. The first experimental points (delay time 0) are taken 20 ps after the laser pulse where heating by the laser can be definitely excluded despite the limited time resolution. Figure 4 depicts cooling curves for different samples and excitation densities. The cooling data are analyzed by comparison with curves calculated with a computer (lines). The algorithm of this program is explained below.

Figure 5 shows the ELR of the different scattering processes as a function of the temperature of the carrier system for low carrier density (calculated after Ref. 2). The deformation potential of the holes is $E^h_{AC}=5.5$ eV, the lowest value obtained by our fits. For temperatures above about 45 K, the PO scattering with LO phonons (Fröhlich interaction) is dominant. The nonpolar optical scattering with TO phonons is about 1 order of magnitude weaker in this temperature range. At low carrier temperatures, the ADP scattering is most important. Piezoelectric scattering with acoustic phonons is only important in the temperature range below 20 K, which is not discussed in our case. In the computer program, only the energy loss by PO scattering and ADP scattering is taken into account.

The ELR for these two scattering processes is calculated using the formulas given in Ref. 2. The PO ELR is given by

$$\left[\frac{dE}{dt}\right]_{PO}=\frac{e^2m^2kT}{K\hbar^5\pi^2}\left[\frac{1}{\epsilon_\infty}-\frac{1}{\epsilon_0}\right](\hbar\omega_{LO})^2[N_{LO}(T_C)-N_{LO}(T_L)]\times\int_0^\infty dq\frac{q^3}{(q^2+q_D^2)^2}\ln\left[\frac{1+\exp[(-\hbar^2/8mkT_C)(q-2m\omega_{LO}/\hbar q)^2+\eta]}{1+\exp[(-\hbar^2/8mkT_C)(q+2m\omega_{LO}/\hbar q)^2+\eta]}\right], \quad (3)$$

where q is the phonon wave vector, m is the electron or hole effective mass, η is the electron or hole Fermi level, T_C is the carrier temperature, T_L is the lattice temperature, and N_q is the phonon occupation probability given by

$$N_q(T)=\frac{1}{\exp(\hbar\omega_q/kT)-1}. \quad (4)$$

The factor K accounts for the reduced overlap of the p-like wave functions of holes compared to the s-like wave functions of electrons. K is set equal to one for electrons. For holes, we use a value of $K=2$.[41] The Debye screening length q_D is given by

$$q_D^2=\frac{8\pi e^2}{\epsilon_\infty kT}\frac{1}{v}\sum_{k,\lambda}\{f^\lambda(k,\eta_i)-[f^\lambda(k,\eta_i)]^2\}, \quad (5)$$

where v is the crystal volume and $f^{\lambda}(k,\eta_i)$ is the Fermi-Dirac function of an electron (hole) in the band λ with Fermi level η_e (η_h). The sum is over all electron (hole) states k. The meanings of the other symbols and the numerical values used for our calculations are given in Table II.

The ADP ELR is given by the relation[2]

$$\left[\frac{dE}{dt}\right]_{\mathrm{ADP}} = \frac{m^2 kTE_{\mathrm{AC}}^2}{4\pi^3 h^3 \rho}\int_0^{\infty} dq \frac{q^7}{(q^2+q_D^2)^2}[N_q(T_C)-N_q(T_L)]\ln\left[\frac{1+\exp[(-\hbar^2/8mkT_C)(q-2mc/\hbar)^2+\eta]}{1+\exp[(-\hbar^2/8mkT_C)(q+2m_c/\hbar)^2+\eta]}\right], \quad (6)$$

where E_{AC} is the acoustic deformation potential. The values of E_{AC}^e and E_{AC}^h for electrons and holes used for the calculations are discussed in Sec. IV D. For further explanation of symbols and numerical values of constants, see Table II.

The cooling curve is now calculated as follows: The algorithm starts with the (experimentally determined) initial carrier temperature T_C^0 (20 ps after the maximum of the laser pulse) and the Fermi level η_e and η_h describing the electron and hole density, respectively. The initial mean energies $\bar{E}_{e,h}$ for electrons and holes, respectively, are calculated using the expressions

$$\bar{E}_{e,h} = \tfrac{3}{2}kTF_{3/2}(\eta_{e,h})/F_{1/2}(\eta_{e,h}) \quad (7)$$

for 3D systems and

$$\bar{E}_{e,h} = kTF_1(\eta_{e,h})/F_0(\eta_{e,h}) \quad (8)$$

for 2D systems. $F_i(\eta)$ is the ith Fermi integral defined as usual.[42] Then the energy-loss by PO [Eq. (3)] and ADP [Eq. (6)] scattering is calculated separately for electrons and holes and subtracted from the mean energies. After this step, the electron and hole systems have different temperatures due to the differences in the ELR of the two carrier types. We assume instant thermalization to a common temperature by exchange of an energy portion ΔE.[43] Finally, the carrier density is reduced according to an exponential carrier density decay with a carrier lifetime τ_c. The Fermi levels η_c and η_h are recalculated using the new density and temperature. Then the procedure is repeated with the new T_C and η_e, η_h as initial values. Using this procedure, we include recombination heating,[43,44] which significantly influences the cooling curves of samples with short carrier lifetimes at higher excitation density. The changes in scattering rate due to degeneracy and the dependence of the specific heat on degeneracy are also included in the algorithm.

The fit procedure is performed as follows. First, the deformation potential E_{AC} entering into the ADP scattering rate is determined by analyzing the low-temperature range (<45 K) of the cooling curve, where scattering with optical phonons is not important. Due to the small effective mass of electrons, the ADP ELR is mainly determined by the scattering of holes, even for the n-type doped samples. We therefore treat only the hole deformation potential E_{AC}^h as a free parameter; for the electron deformation potential E_{AC}^e we use 7.0 eV. After the determination of the hole deformation potential, the higher-temperature part of the curves is analyzed. As ob-

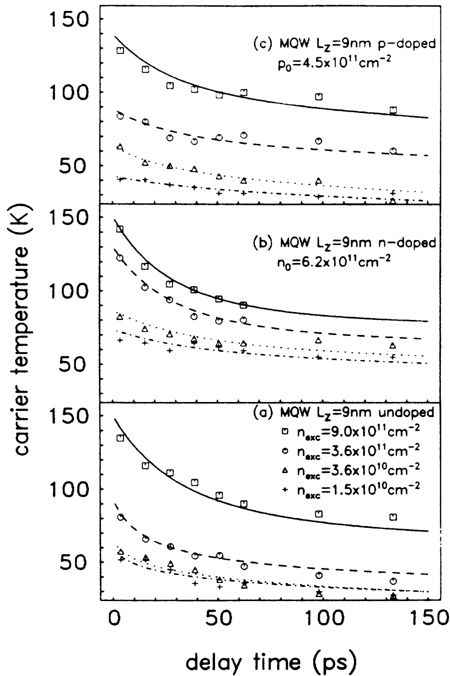

FIG. 4. Cooling curves for differently doped 9-nm QW. The symbols are the experimentally determined plasma temperatures. The lines are fits calculated with the code described in the text. The zero delay time is set to 20 ps after the maximum of the laser pulse.

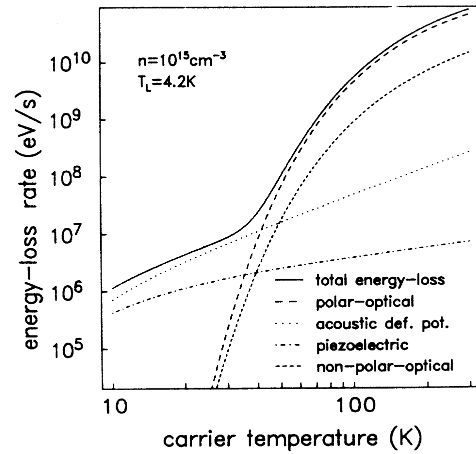

FIG. 5. Energy-loss rates per carrier by the different scattering mechanisms as a function of the carrier temperature. The solid line is the sum of the four interactions. The acoustic deformation-potential scattering is calculated with a hole deformation potential E_{AC}^h=5.5 eV and an effective mass m_h=0.5m_0.

TABLE II. Constants used for the calculations. All data are from Ref. 45, except the values marked by a superscript.

Symbol	Meaning	Numerical value
m_e^*	electron effective mass	$0.067m_0$
m_h^*	hole effective mass	$0.5m_0$
ϵ_0	static dielectric constant	12.75
ϵ_∞	optical dielectric constant	10.94
$\hbar\omega_{\mathrm{LO}}$	LO-phonon energy	36.4 meV
E_{AC}^e	electron deformation potential	7.0 eV[a]
E_{AC}^h	hole deformation potential	5.5–8 eV[b]
ρ	density of GaAs	5.32 $\mathrm{g/cm^3}$
c	sound velocity	3.57×10^5 cm/s[c]

[a]From D. L. Rode, Phys. Rev. B **2**, 1012 (1970).
[b]See discussion in Sec. IV D.
[c]From T. B. Bateman *et al.*, J. Appl. Phys. **30**, 544 (1959).

served generally, the experimentally determined PO ELR, $(dE/dt)_{\mathrm{expt}}$, is, at least at high excitation density, reduced independently of delay time compared to the theoretically expected energy loss PO ELR, $(dE/dt)_{\mathrm{theor}}$, calculated with the simple theory of the Fröhlich interaction (no hot phonons, no screening). We define a reduction parameter α, which describes the reduction of the experimental energy loss compared to the theoretical energy loss:

$$\left[\frac{dE}{dt}\right]_{\mathrm{expt}}=\left[\frac{dE}{dt}\right]_{\mathrm{theor}}\Big/\alpha\ . \tag{9}$$

We deliberately do not use a phenomenological scattering time τ_{PO} or τ_{av} to avoid confusion with the scattering rate of a single carrier with a LO phonon. The cooling curve is then fitted treating α as a free parameter. At low excitation density, α describes the PO ELR due to the Fröhlich interaction as a function of doping, dimensionality, and well width. It has been shown[5,6] for bulk GaAs that the PO ELR at high excitation density is strongly influenced by the scattering with TO phonons due to their lower sensitivity to hot-phonon effects. With our experimental method it is not possible to separate the contributions of polar optical and nonpolar optical scattering due to their very similar temperature dependence (see Fig. 5). In the high-density limit, α therefore includes both interactions. We use for the analysis of bulk GaAs as well as for QW's the 3D PO ELR [Eq. (3)] and ADP ELR [Eq. (6)]. Thereby, the reduction of the PO ELR expressed by α uses the 3D case as a reference. For the calculation of the PO ELR energy loss, we set $q_D=0$, i.e., we include the effect of screening in α. We prefer this method over the use of any screening theory for PO scattering, because different theoretical approaches to the effect of screening yielded results differing by more than an order of magnitude.[2,4,8]

IV. RESULTS AND DISCUSSION

A. Undoped quantum wells and bulk GaAs

The values for the PO ELR for bulk GaAs and the undoped QW's of different well width are given in Fig. 6(a) as a function of the *volume* excitation density $n_{\mathrm{exc}}^{3\mathrm{D}}$. In the limit of low excitation density, the PO ELR comes close to the simple theory of the Fröhlich interaction (no screening, no hot phonons, 3D) *independent of dimensionality and well width.* At higher excitation density, the PO ELR is reduced by up to more than 2 orders of magnitude. For bulk GaAs and the 20-nm QW, the dependence on excitation density is equal within error. The 9-nm QW, however, and—much more pronounced—the 3-nm QW show a lower reduction of the PO ELR with increasing $n_{\mathrm{ex}}^{3\mathrm{D}}$. At first sight, one could presume a dependence of the PO ELR reduction on the quantum-well width. However, for QW's the *sheet* density is the appropriate parameter, since in QW's a two-dimensional carrier system is interacting with a two-dimensional phonon system.[30] No dependence of the PO ELR on the well width is obtained if one plots the PO ELR as a function of the *sheet* excitation density $n_{\mathrm{exc}}^{2\mathrm{D}}$ [Fig. 6(b)]. We thus conclude (i) that the Fröhlich interaction is independent, within experimental error, of dimensionality and well width, and (ii) that the reduction of the PO ELR at high

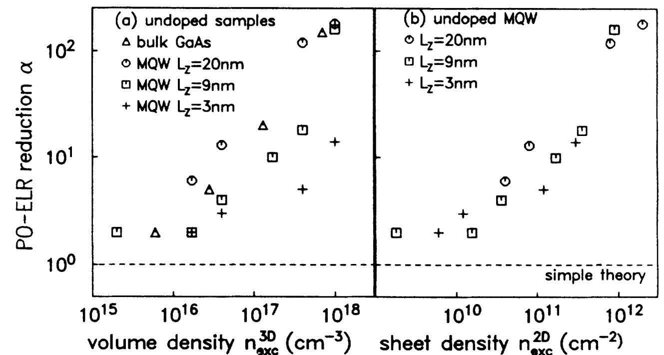

FIG. 6. (a) The PO ELR reduction factor α for the undoped MQW as a function of the *volume* excitation density $n_{\mathrm{exc}}^{3\mathrm{D}}$. The values for the undoped bulk sample are shown for comparison. The dashed line is the result expected by the simple theory of the Fröhlich interaction (no screening, no hot phonons, 3D). (b) The PO ELR reduction factor α for the undoped MQW as a function of the *sheet* excitation density $n_{\mathrm{exc}}^{2\mathrm{D}}$.

excitation densities is independent of dimensionality and well width and scales with the *sheet* excitation density.

We have already mentioned that in the 20-nm QW higher subbands are involved in the cooling process. The carriers are excited into the $n=1$ to $n=3$ subbands during the laser pulse. Within our time resolution, we observe no luminescence from the $n=3$ subband edge, indicating a rapid relaxation of the carriers (or, at least, of one type of carriers) into lower subbands. This is expected due to the short intersubband relaxation times for subband edges more than a LO-phonon energy apart.[46] The luminescence spectra indicate that the $n=2$ subband is (at the highest excitation density of our experiments) occupied by carriers thermalized with the $n=1$ subband. At lower excitation densities, we always observe only luminescence from thermalized carriers in the lowest subbands. The electron relaxation time between the $n=2$ and $n=1$ subbands should be several hundred ps,[47] since the subband edges are separated by less than one LO-phonon energy. This slow relaxation of carriers could act as a persistent heating effect. However, it is obvious from Fig. 6(b) that the cooling behavior of the 20-nm QW is within error identical to that of the narrower QW, indicating that the effect of higher subbands on the cooling is rather small.

In undoped samples, we always observe the combined effects of electron and hole relaxation. The investigation of doped samples, which allows us to study the difference in cooling behavior of electrons and holes, is discussed in the next subsection.

B. Modulation-doped quantum wells

The doped MQW's used in these experiments have a doping density in the range 6×10^{11} cm^{-2} to 1.2×10^{12} cm^{-2} for the n-type doped samples and 4.5×10^{11} cm^{-2} to 6×10^{11} cm^{-2} for the p-type doped samples. At the lowest excitation densities ($n_{exc}^{2D}\approx10^{10}$ cm^{-2}) the plasma consists mainly of one component, and the carrier-phonon coupling can be studied separately for electrons and holes. In the high-excitation limit, the excitation density is higher than the doping density which should lead to a similar PO ELR as in the undoped samples.

Figures 7 and 8 show the PO ELR as a function of the *sheet* excitation density n_{exc}^{2D} for the n- and p-type samples. Obviously, the cooling is strikingly different for electrons and holes. Electrons show even at very low excitation density a PO ELR rate which is reduced by more than an order of magnitude. This reduction depends on the doping density. The 9-nm QW with slightly higher (1.2×10^{12} cm^{-2}) doping than the 20- and 3-nm QW's (8 and 6.2×10^{11} cm^{-2}, respectively) has a slightly lower PO ELR at low excitation densities, where the plasma consists mainly of electrons.

Holes show a similar behavior of the energy loss as a function of the excitation density as the EHP in the undoped samples, indicating that the cooling of an EHP with a similar concentration of electrons and holes is dominated by the energy loss of the holes. At low *excitation* density, holes come close to the theory of the Fröhlich interaction ($\alpha=1.5\pm0.5$), although the *doping*

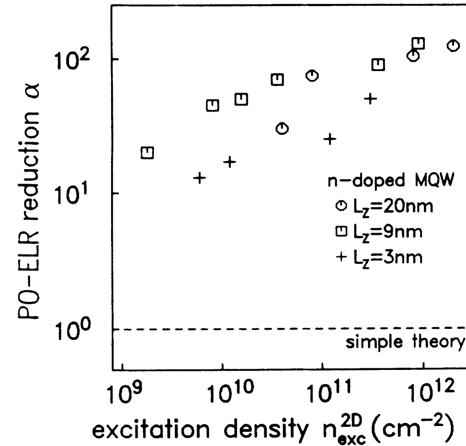

FIG. 7. The PO ELR reduction factor α as a function of the *sheet excitation* density n_{exc}^{2D} for the n-type doped QW's. The dashed line shows the result expected by the simple theory of the Fröhlich interaction.

densities p_0 are in the range of 5×10^{11} cm^{-2} (or, expressed as volume density, up to 1.3×10^{18} cm^{-3}). We therefore conclude that the reduction of the PO ELR observed is up to this density *not caused by screening*. Similarly, degeneracy can be ruled out, because at the hole densities in our samples the Fermi level is already above the band edge.

Two of the possible reasons for the difference between electrons and holes are as follows: (i) Electrons do not interact with TO phonons by nonpolar optical scattering. Calculations of Pötz and Kocevar[5] for bulk GaAs have shown that the energy loss due to TO-phonon scattering is much less influenced by hot phonons than the PO ELR. However, in the low-density limit, holes come close to the PO ELR predicted by the Fröhlich interaction without the effect of screening or hot phonons. This PO ELR is about 1 order of magnitude greater than the nonpolar optical scattering with TO phonons. This

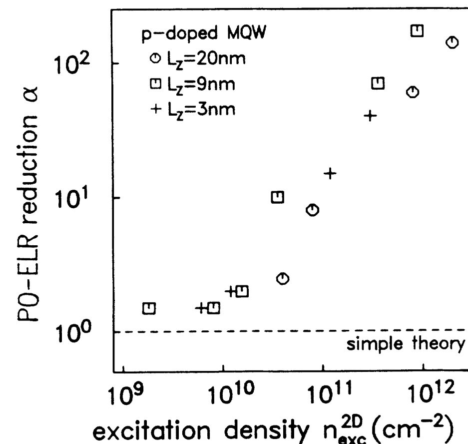

FIG. 8. The PO ELR reduction factor α as a function of the *sheet excitation* density n_{exc}^{2D} for the p-type doped QW's.

demonstrates that the different behavior of electrons and holes is at least in the low-density limit not caused by TO-phonon scattering. (ii) Due to their smaller effective mass, the electrons interact with phonons having q vectors which are about a factor of $(m_h^*/m_e^*)^{1/2} \approx 2.6$ smaller than for the holes. The 2D electron gas in a QW has two degrees of freedom, i.e., the q-vector area influenced by the interaction with the electrons is ≈ 7 times smaller than for holes. A reduction of the PO ELR due to hot phonons should therefore be equivalent for (*two-dimensional*) electrons and holes, if the carrier density of the electrons is about a factor of 7 smaller.

C. Comparison with a hot-phonon model

We now estimate the critical density n_{crit} at which the PO ELR of an electron gas starts to be reduced by an optical-phonon overpopulation. For simplicity, we neglect screening and degeneracy. Their influence on the reduction of the PO ELR is small, as discussed in the preceding subsection. The electrons emit (in the temperature range of our experiment) LO phonons with wave vectors in the range between about 1×10^6 cm^{-1} and 4×10^6 cm^{-1} (Ref. 18). These are only about 1.2×10^{-3} of the LO-phonon modes in a 2D Brillouin zone, i.e., the relevant phonon states have a sheet density of about $n_{\mathrm{LO}}^{\mathrm{rel}} = 2.0\times10^{12}$ cm^{-2}. We describe the (over-) population of this phonon-vector range by a phonon temperature T_P which is higher than the lattice temperature T_L and lower than the carrier temperature T_C. In the limit of Maxwell-Boltzmann statistics and for T_L, T_C, and $T_P < \Theta = \hbar\omega_{\mathrm{LO}}/k$ the reduced PO ELR is given by

$$\left.\frac{dE}{dt}\right|_{\mathrm{red}} = \frac{\hbar\omega_{\mathrm{LO}}}{\tau_{\mathrm{PO}}}[\exp(-\Theta/T_C) - \exp(-\Theta/T_P)] , \quad (10)$$

which relates to the undisturbed PO ELR

$$\left.\frac{dE}{dt}\right|_{T_P \ll T_C} = \frac{\hbar\omega_{\mathrm{LO}}}{\tau_{\mathrm{PO}}}\exp(-\Theta/T_C) \quad (11)$$

by the equation

$$\alpha\left.\frac{dE}{dt}\right|_{\mathrm{red}} = \left.\frac{dE}{dt}\right|_{T_P \ll T_C} , \quad (12)$$

where τ_{PO} is the scattering time with a LO phonon averaged over a Maxwell-Boltzmann distribution. In some experimental work, this time was treated as a free parameter and used to express the PO ELR reduction. Here, we use the theoretical value, which is in the order of 0.1 ps for both electrons and holes. The reduction of the PO ELR expressed by α included only the effect of hot phonons in this context.

We obtain from Eqs. (10)–(12)

$$T_P = \frac{T_C}{1-(T_C/\Theta)\ln(1-1/\alpha)} . \quad (13)$$

We now first consider a steady-state equilibrium, where the excitation and annihilation of LO phonons are equal. In this case, n electrons have a net emission of

$$\frac{n}{\tau_{\mathrm{PO}}}[\exp(-\Theta/T_C) - \exp(-\Theta/T_P)] = \frac{n_{\mathrm{LO}}^{\mathrm{rel}}}{\tau_{\mathrm{LO}}}\exp(-\Theta/T_P) , \quad (14)$$

where the right-hand side describes the anharmonic decay of $n_{\mathrm{LO}}^{\mathrm{rel}}\exp(-\Theta/T_P)$ ($T_P < \Theta$) phonons with lifetime τ_{LO} into acoustical phonons. We neglect the temperature and energy dependencies of τ_{LO} and τ_{PO}, which are small in the range considered here. After some algebra we obtain from Eqs. (13) and (14)

$$\alpha = 1 + \frac{n}{n_{\mathrm{LO}}^{\mathrm{rel}}}\frac{\tau_{\mathrm{LO}}}{\tau_{\mathrm{PO}}} . \quad (15)$$

This equation gives valuable information. (i) The reduction of α is only a function of density and not of T_C or T_P. This explains why in our non-steady-state but time-resolved experiment we are able to fit our experimental curves (after an initial distortion which we have to omit due to the limited time resolution) with a constant α for each density, which is independent of T_C and the phonon overpopulation (i.e., T_P). The situation resembles a quasi-steady-state case. (ii) At a critical density $n_{\mathrm{crit}} = n_{\mathrm{LO}}^{\mathrm{rel}}\tau_{\mathrm{PO}}/\tau_{\mathrm{LO}}$, the PO ELR is reduced to half of the low-density limit (i.e., $\alpha = 2$). For $n \ll n_{\mathrm{crit}}$, the PO ELR is undisturbed by hot phonons ($\alpha = 1$), for $n \gg n_{\mathrm{crit}}$, α increases linearly with the carrier density. Using typical values [$\tau_{\mathrm{PO}} = 0.1$ ps, $\tau_{\mathrm{LO}} = 10$ ps (Ref. 48)], we obtain for electrons $n_{\mathrm{crit}} = 2\times10^{10}$ cm^{-2}.

The n-type samples of our experimental have a doping density much greater than that. It is therefore not surprising that we do not reach the bare Fröhlich interaction (i.e., $\alpha = 1$) even for the lowest excitation density. If we calculate the lower bound for α caused by the doping densities in our n-type doped samples, we obtain $\alpha \approx 50$ for the 9-nm QW, $\alpha \approx 40$ for the 20-nm QW, and $\alpha \approx 20$ for the 3-nm QW, in rather good agreement with our experimental findings.

The critical density for holes is about a factor of 7 higher ($n_{\mathrm{crit}} = 1.4\times10^{11}$ cm^{-2}) owing to their much larger mass. We would expect $\alpha \approx 3$ as a lower bound for the given doping densities. Experimentally, we observe lower values $\alpha = 1.5 \pm 0.5$. The high-density limit follows the linear behavior predicted by the model. A detailed quantitative comparison between experiment and this model is not possible, since some rather crude approximations are made: The interaction with phonons depends on the q vector, which leads to a dependence of T_P on q neglected in our model. Furthermore, we have used Maxwell-Boltzmann statistics, which is especially questionable for electrons at higher densities, and we have neglected nonpolar optical scattering.

D. Deformation-potential scattering

In the low-temperature regime ($T_C < 40$ K), the ELR is determined by acoustic deformation-potential scattering. Two parameters enter critically into the ADP ELR—the effective mass m^* and the deformation-potential constant E_{AC}:

$$\left[\frac{dE}{dt}\right]_{\mathrm{ADP}} \propto (m^*)^{5/2} E_{\mathrm{AC}}^2 \ . \qquad (16)$$

Since $E^e_{\mathrm{AC}} \approx E^h_{\mathrm{AC}}$, the ADP ELR of holes dominates by far over the ADP ELR of electrons due to the much smaller effective mass of electrons. The ADP ELR is determined by fitting the low-density cooling curves in the low-temperature range. The values obtained are used for all curves of higher density. We observe no difference between doped and undoped QW's. For an easier comparison with literature, we have assumed a constant hole mass ($m_h^* = 0.5m_0$) and varied the deformation potential E^h_{AC} in our analysis. In bulk GaAs and in the 20-nm QW, $E^h_{\mathrm{AC}} = 5.5$ eV is obtained. This value of E^h_{AC} is in reasonable agreement with the values of 4.8 eV obtained without screening of the ADP scattering.[33,34,43] For the narrower QW, however, we observe an increase in ADP scattering. For the 9- and 3-nm QW's, the ADP ELR increases by a factor of about 1.6 and 2.1, respectively (Fig. 9). We cannot decide whether the differences in the ADP ELR are caused by an increase in the deformation-potential constant or by a change in the effective mass due to the complicated dependence of the valence-band structure on the QW width.[49]

V. COMPARISON WITH EARLIER RESULTS AND THEORY

The results of Shah *et al.*[18] obtained with cw luminescence and electrical heating are in good agreement with our results obtained in the low-excitation-density region. A calculation of the PO ELR in Ref. 18 using a 3D model supports the explanation of the reduced PO ELR by a hot-phonon effect. The samples used by Yang *et al.*[19] had a doping density more than a factor of 2 lower than ours, but still much higher than the critical density estimated in Sec. IV C. Therefore, their result seems to be incompatible with ours. However, a comparison with a sample with the same doping density would help to clarify this controversy.

The determination of PO ELR rates in undoped GaAs QW by time-resolved luminescence experiments have shown rather contradictory results up to now. Shank *et al.*[15] obtained the same PO ELR for bulk GaAs and GaAs QW's at the same *volume density*. Uchiki *et al.*[21] observed at one excitation density a strong reduction of the PO ELR, which they mainly ascribed to the different properties of a 2D system. Recently, they have studied[29] QW's of different well widths. However, they give no experimental results concerning the PO ELR for different well widths. We obtain at a given volume density a *lower* reduction of the PO ELR in a 3-nm QW, which, however, disappears if we use the *sheet* density as the appropriate parameter for 2D systems. Recently, Tatham *et al.*[32] have obtained similarly an increased PO ELR for a narrow (2.5 nm) GaAs QW compared to a 6-nm QW at a given *volume* density. They explained this result by a reduced influence of hot phonons, because the relaxation of momentum conservation perpendicular to the GaAs layer allows the carriers to couple with a larger number of phonon modes. However, the increased PO ELR could be probably explained similarly to our work, if the *sheet* density is used instead of the *volume* density. Obviously, the description by the volume density is inappropriate for narrow QW.

For a comparison with theory, one has to consider the low- and the high-density regimes.

(i) The influence of dimensionality and well width on the Fröhlich interaction *in the low-density* limit (no hot phonons, no screening) has been addressed by several authors. Generally, only a weak dependence of the scattering rate on the reduced dimensionality has been expected. Riddoch and Ridley[11] have predicted that the scattering rate is only slightly changed in QW's compared to the bulk. However, these calculations are done for electrons. We reach the low-density PO ELR only for the *p*-type samples; for *n*-type samples the PO ELR is strongly reduced even at our lowest excitation density. Theoretical calculations for holes are, to our knowledge, not available. They are rather difficult due to the complicated valence-band structure in 2D systems.

(ii) A calculation by Cai *et al.*[12] indicates that the reduction of the PO ELR *at high densities* by hot phonons is rather insensitive to the dimensionality in agreement with our results. A recent Monte Carlo calculation by Lugli and Goodnick[13] came to the conclusion that the PO ELR reduction for a given *sheet* density is independent of well width, consistent with our results. Earlier experimental data given in Ref. 23 are in contrast to this prediction.

The first experimental results for *n*-type doped GaAs QW's were given by Ryan *et al.*[17] They observed a reduction of the PO ELR by a factor of 60 (compared to the simple theory) *independent* of excitation density, in contrast to the excitation density dependence observed in undoped bulk GaAs. This was explained by the different properties of the electron-phonon interaction in 2D systems. However, a comparison of the results for *n*-type doped and *p*-type doped QW's (see Figs. 7 and 8) shows that the effect observed in Ref. 17 was most probably caused by the *n*-type doping, as recently observed in InGaAs.[26] The results might have been further distorted by the excitation of the barriers. Later measurements[23] with excitation only into the wells yielded a different result.

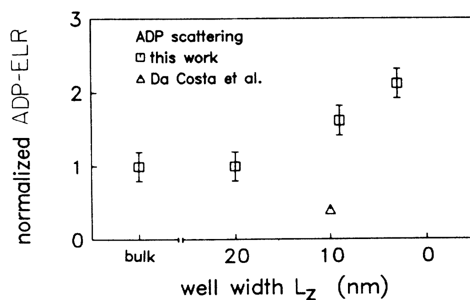

FIG. 9. The ADP ELR as a function of the QW width L_z, normalized to the bulk ADP ELR ($E^h_{\mathrm{AC}} = 5.5$ eV, $m_h = 0.5m_0$). The triangle shows the value given by Da Costa *et al.* (Ref. 24).

The cooling in p-type GaAs QW's has been investigated by Kash *et al.*[22] The PO ELR decreased with increasing excitation density, but was independent of doping density. We cannot confirm this result with our data, since the doping densities of our p-type samples are nearly identical. Our measurements with n-type samples, however, are dependent on doping density.

By comparison with the simple theory of the Fröhlich interaction, Kash *et al.*[22] concluded that the reduction of the PO ELR is *dependent* on the delay time, i.e., a description by a time-independent scattering time τ_{PO} or reduction factor α is *not* justified. However, they neglected several important effects in their analysis, e.g., acoustic deformation-potential scattering, degeneracy, and recombination heating. An analysis of their cooling curves for the highly doped sample ($p_0 = 4\times10^{17}$ cm^{-3}) performed with our algorithm shows a good agreement with a *time-independent* reduction of the PO ELR, as we expect according to our model in Sec. IV C. The main reason for the different results is the neglect of ADP scattering, which leads to an overestimation of optical-phonon scattering in the low-temperature range. We have additionally fitted the luminescence spectra in Ref. 22 and obtained excitation densities a factor of 2 higher than stated in Ref. 22. Figure 10 shows the values of α obtained by an analysis of the cooling curves of Ref. 22 in comparison to our results for a 9-nm QW with similar doping density.

The dependence of the acoustic deformation-potential scattering on the QW width was reported first by us.[31] In the literature, the only determination of the hole deformation potential E^h_{AC} in a GaAs QW is reported in Ref. 24. A value of $E^h_{AC} = 3.5$ eV was obtained, marked by a triangle in Fig. 9 (assuming a hole mass $m_h = 0.5m_0$). This E^h_{AC} is significantly less than the value we have obtained in bulk GaAs using an analysis with unscreened ADP scattering[43,50] or in the present measurement ($E^h_{AC} = 5.5$ eV). The difference compared to our result for a 9-nm QW ($E^h_{AC} = 7.0$ eV) is even greater. The origin of this discrepancy is not clear.

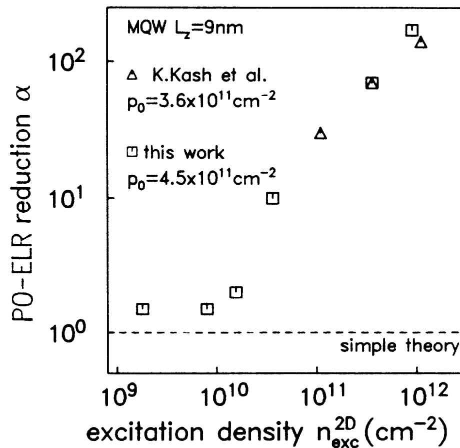

FIG. 10. The PO ELR reduction factor α as a function of the *sheet excitation* density n^{2D}_{exc} for 9-nm p-type doped QW's. The squares are results of this work. The triangles are obtained by analysis of the cooling curves given by K. Kash *et al.* (Ref. 22) with the theoretical model described in this paper. The excitation densities obtained by a fit of the luminescence spectra of Ref. 22 are a factor of 2 greater than stated there. For this plot, we have used the densities obtained by the fit. The dashed line gives the PO ELR due to the bare 3D Fröhlich interaction.

The PO ELR at low electron densities and temperatures might be influenced by plasmon scattering as discussed by Das Sarma and co-workers.[8,9] In our case, however, ADP scattering is important only in the presence of holes, and inter-valence-band absorption of holes is a strong damping process for plasmons. We therefore expect that the energy is actually not dissipated into the plasmon system, but remains in the carrier system.

Recently, Hirakawa and Sakaki[51] have studied the scattering of electrons in a GaAs/$Al_xGa_{1-x}As$ heterojunction in the low-temperature regime. The energy loss was determined by acoustic deformation-potential scattering. The deformation-potential constant obtained was 11 eV, significantly higher than the commonly accepted value for bulk GaAs of 7 eV.[52] It is possible that the increase in the ADP ELR observed by us is also caused by an increase in E^h_{AC}; however, it might also result from a change of the in-plane mass due to the confinement.

VI. CONCLUSION

We have systematically studied the cooling of hot carriers in undoped, n-type doped, and p-type doped GaAs QW's and bulk GaAs by time-resolved luminescence. We obtain a detailed picture of the dependence of the energy-loss rate by LO phonons, PO ELR, on the various parameters. The main results are the following: At high excitation density, the energy-loss rates of electrons and holes are reduced *independently of the delay time.* This reduction of the PO ELR is independent of dimensionality and well width if the *sheet* density is used as the appropriate parameter. At low excitation density, holes come close to the simple theory of the Fröhlich interaction. Electrons, however, have still a reduced PO ELR. Above a critical density, the PO ELR decreases linearly with the density. We give a simple model of the cooling including the hot-phonon effect, which qualitatively explains these findings. Screening or degeneracy, however, can be ruled out as reasons for the reduction of the PO ELR. The energy loss due to deformation-potential scattering with acoustical phonons, ADP ELR, which is most important in the low-temperature regime, increases with decreasing well width.

ACKNOWLEDGMENTS

We are indebted to E. Bauser for providing the bulk GaAs sample, H. J. Queisser for his participation in this work, and T. Reinecke and D. Broido for providing unpublished results. We thank P. Kocevar, H. J. Polland, and H. Lobentanzer for fruitful discussions about hot-

carrier cooling. Discussions with G. Tränkle, E. Lach, and A. Forchel about calculations of luminescence spectra were of great help. We thank M. Hauser, K. Rother, and H. Klann for expert technical assistance, and J. Kuhl for a critical reading of the manuscript and many helpful suggestions. The financial support by the Bundesministerium für Forschung und Technologie, is gratefully acknowledged.

[1]S. Lyon, J. Lumin. **35**, 121 (1986).
[2]M. Pugnet, J. Collet, and A. Cornet, Solid State Commun. **38**, 531 (1981).
[3]J. Shah, IEEE J. Quantum Electron. **QE-22**, 1728 (1986).
[4]E. J. Yoffa, Phys. Rev. B **23**, 1909 (1981).
[5]W. Pötz and P. Kocevar, Phys. Rev. B **28**, 7040 (1983).
[6]P. Kocevar, Festkörperprobleme (*Advances in Modern Physics*), edited by P. Grosse (Vieweg, Braunschweig, 1987), Vol. 27, p. 197.
[7]E. Vass, Z. Phys. B **67**, 435 (1987).
[8]S. Das Sarma, J. K. Jain, and R. Jalabert, Proceedings of the 5th International Conference on Hot Carriers in Semiconductors, Boston, 1987 [Solid State Electron. **31**, 695 (1988)].
[9]S. Das Sarma, J. K. Jain, and R. Jalabert, Phys. Rev. B **37**, 6290 (1988).
[10]C. H. Yang and S. A. Lyon, Physica B + C **134B**, 305 (1985).
[11]F. A. Riddoch and B. K. Ridley, J. Phys. C **16**, 6971 (1983).
[12]W. Cai, M. C. Marchetti, and M. Lax, Phys. Rev. B **35**, 1369 (1987).
[13]P. Lugli and S. M. Goodnick, Phys. Rev. Lett. **59**, 716 (1987).
[14]P. J. Price, Physica B + C **134B**, 164 (1985).
[15]C. V. Shank, R. L. Fork, R. Yen, J. Shah, B. I. Greene, A. C. Gossard, and C. Weisbuch, Solid State Commun. **47**, 981 (1983).
[16]Z. Y. Xu and C. L. Tang, Appl. Phys. Lett. **44**, 692 (1984).
[17]J. F. Ryan, R. A. Taylor, A. J. Turberfield, A. Maciel, J. M. Worlock, A. C. Gossard, and W. Wiegmann, Phys. Rev. Lett. **53**, 1841 (1984).
[18]J. Shah, A. Pinczuk, A. C. Gossard, and W. Wiegmann, Phys. Rev. Lett. **54**, 2045 (1985).
[19]C. H. Yang, J. M. Carlson-Swindle, S. A. Lyon, and J. M. Worlock, Phys. Rev. Lett. **55**, 2359 (1985).
[20]J. Shah, A. Pinczuk, A. C. Gossard, and W. Wiegmann, Physica B + C **134B**, 174 (1985).
[21]H. Uchiki, T. Kobayashi, and H. Sakaki, Solid State Commun. **55**, 311 (1985).
[22]K. Kash, J. Shah, D. Block, A. C. Gossard, and W. Wiegmann, Physica B + C **134B**, 189 (1985).
[23]J. F. Ryan, R. A. Taylor, A. J. Turberfield, and J. M. Worlock, Surf. Sci. **170**, 511 (1986).
[24]J. A. P. Da Costa, R. A. Taylor, A. J. Turberfield, J. F. Ryan, and W. I. Wang, in *Proceedings of the International Conference on the Physics of Semiconductors, Stockholm, 1986*, edited by O. Engström (World Scientific, Singapore, 1987), p. 1327.
[25]H. Lobentanzer, W. W. Rühle, W. Stolz, and K. Ploog, Solid State Commun. **62**, 53 (1987).
[26]H. Lobentanzer, W. W. Rühle, H. J. Polland, W. Stolz, and K. Ploog, Phys. Rev. B **36**, 2954 (1987).
[27]H. J. Polland, W. W. Rühle, J. Kuhl, K. Ploog, K. Fujiwara, and T. Nakayama, Phys. Rev. B **35**, 8273 (1987).
[28]H. J. Polland, W. W. Rühle, K. Ploog, and C. W. Tu, Phys. Rev. B **36**, 7722 (1987).
[29]H. Uchiki, Y. Arakawa, H. Sakaki, and T. Kobayashi, J. Appl. Phys. **62**, 1010 (1987).
[30]K. Leo, W. W. Rühle, H. J. Queisser, and K. Ploog, Phys. Rev. B **37**, 7121 (1988).
[31]K. Leo, W. W. Rühle, H. J. Queisser, and K. Ploog, Appl. Phys. A **45**, 35 (1988).
[32]M. Tatham, R. A. Taylor, J F. Ryan, W. I. Wang, and C. T. Foxon, in Proceedings of the 5th International Conference on Hot Carriers in Semiconductors, Ref. 8, p. 459.
[33]W. W. Rühle, H. J. Polland, E. Bauser, K. Ploog, and C. W. Tu, in Proceedings of the 5th International Conference on Hot Carriers in Semiconductors, Ref. 8, p. 407.
[34]W. W. Rühle, H. J. Polland, and K. Leo, *Proceedings of the International Conference on the Physics of Semiconductors*, Ref. 24, p. 211.
[35]J. S. Blakemore, J. Appl. Phys. **53**, R123 (1982).
[36]Y. Masumoto, M. Matsuura, S. Tarucha, and H. Okamoto, Phys. Rev. B **32**, 4275 (1985).
[37]G. Tränkle, H. Leier, A. Forchel, and G. Weimann, Surf. Sci. **174**, 211 (1986).
[38]P. T. Landsberg, Phys. Status Solidi **15**, 623 (1966).
[39]T. Reinecke and D. Broido (unpublished).
[40]W. W. Rühle, K. Leo, and N. M. Haegel, in *Proceedings of the 14th International Conference on GaAs and Related Compounds, Heraklion, 1987,* edited by A. Christou and H. S. Rupprecht, Institute of Physics Conference Series 91 (IOP Bristol, 1988), p. 105.
[41]E. O. Göbel and O. Hildebrand, Phys. Status Solidi **B88**, 645 (1978).
[42]K. Seeger, *Semiconductor Physics,* 2nd ed. (Springer-Verlag, Berlin, 1982).
[43]K. Leo and W. W. Rühle, Solid State Commun. **62**, 659 (1987).
[44]D. Bimberg and J. Mycielski, Phys. Rev. B **31**, 5490 (1985).
[45]*Landolt-Börnstein,* New Series, edited by O. Madelung, M. Schulz, and H. Weiss (Springer-Verlag, Berlin, 1982), Vol. 17a.
[46]A. Seilmeier, H. J. Hübner, G. Abstreiter, G. Weimann, and W. Schlapp, Phys. Rev. Lett. **59**, 1345 (1987).
[47]D. Y. Oberli, D. R. Wake, M. V. Klein, J. Klem, T. Henderson, and H. Morkoç, Phys. Rev. Lett. **59**, 696 (1987).
[48]J. A. Kash and J. C. Tsang, Proceedings of the 5th International Conference on Hot Carriers in Semiconductors, Ref. 8, p. 419.
[49]A. Fasolino and M. Altarelli, in *Two-Dimensional Systems, Heterostructures, and Superlattices,* Vol. 53 of *Springer Series in Solid State Sciences,* edited by G. Bauer, F. Kuchar, and H. Heinrich (Springer-Verlag, Berlin, 1984).
[50]W. W. Rühle and H. J. Polland, Phys. Rev. B **36**, 1683 (1987).
[51]K. Hirakawa and H. Sakaki, Appl. Phys. Lett. **49**, 889 (1986).
[52]D. L. Rode, Phys. Rev. B **2**, 1012 (1970).